Existence of α-cluster structure in ^{44}Ti via the (^{6}Li,d) reaction

T. Yamaya and S. Oh-ami
Department of Physics, Tohoku University, Sendai 980, Japan

M. Fujiwara and T. Itahashi
Research Center for Nuclear Physics, Osaka University, Osaka 567, Japan

K. Katori
Department of Physics, Osaka University, Osaka 588, Japan

M. Tosaki
Laboratory of Applied Physics, Kyoto Prefectual University, Kyoto 606, Japan

S. Kato
Faculty of General Education, Yamagata University, Yamagata 990, Japan

S. Hatori
Department of Physics, Kyoto University, Kyoto 606, Japan

S. Ohkubo
Department of Applied Science, Kochi Women's University, Kochi 780, Japan
(Received 30 May 1990)

α-cluster states in ^{44}Ti have been investigated in the ^{40}Ca(^{6}Li,d)^{44}Ti reaction at $E=50$ MeV. The angular distributions of 34 levels at excitation energies for $E_x=0$–13 MeV allow us to analyze the data. The angular distributions of positive-parity members of the ground-state band (the $K^\pi=0^+$ band) in ^{44}Ti were well reproduced by the finite-range distorted-wave Born approximation calculations up to the transferred angular momentum of $L=8$. For the members of the negative-parity band (the $K^\pi=0^-$ band) with the primary quantum number $N=13$, three levels at 6.22, 7.34, and 9.43 MeV were identified as the 1^-, 3^-, and 5^- states, respectively. The existence of a negative-parity band in ^{44}Ti has been investigated for a long time and persistently gives considerable support to α-cluster models for nuclei heavier than $A=40$.

I. INTRODUCTION

In most nuclei lighter than $A=40$, α clustering is a highly prominent feature in a large number of states. A typical example of α clustering in light nuclei is found in ^{20}Ne, where the ^{16}O+α structure is particularly stable. For nuclei heavier than $A=40$, which have a strong effect of the spin-orbit coupling force on nuclear structure, many theoretical and experimental studies have been devoted to the investigation of α clustering. In fp-shell nuclei,[1–9] in particular the nucleus ^{44}Ti, a ^{40}Ca+α structure is predicted to be especially stable. However, α clustering in ^{44}Ti is not as clear as it is in ^{20}Ne where the viewpoint of moleculelike structure has been unambiguously established.[9,10] A key to the establishment of the α-cluster model of ^{44}Ti is to identify clearly which of the negative-parity members of the parity doublet band is a partner of the positive-parity band. These states have been inevitably predicted by the α-cluster theories,[4–8] but have never been experimentally observed in the fp-shell nuclei. Therefore, it is of significance to investigate the members of the negative-partity band in order to firmly establish the α-cluster viewpoint in ^{44}Ti.

Direct experimental evidence for α clustering in ^{44}Ti can be provided by α-transfer reactions on ^{40}Ca. Many experiments of four-nucleon transfer on ^{40}Ca have been done using different reactions[11–21] (^{16}O,^{12}C),[11–14] (^{18}O,^{14}C),[15] (^{20}Ne,^{16}O),[16] and (^{6}Li,d).[17–19] The (^{6}Li,d) reaction is, in particular, a powerful tool for α-clustering study. Experimental studies of the reaction (^{6}Li,d) on ^{40}Ca have been done at incident energies near 30 MeV;[18,19] however the members of the negative-parity band in ^{44}Ti are not evident in these data. The sharp rise in the observed cross sections at backward angles in the elastic ^{40}Ca(α,α_0) scattering experiments[20,21] suggested the presence of α-cluster structure at excitation energies above the α threshold in ^{44}Ti. The ^{40}Ca(α,γ) capture reaction[22–24] and the heavy-ion-induced reactions (HI, X_γ) (Ref. 25) have identified the levels of a band of positive-parity states which begins with the 0^+ ground state and apparently terminates at the 8.04-MeV 12^+ state in ^{44}Ti.

In the present work, the (^{6}Li,d) reaction on ^{40}Ca has been used to investigate the members of the negative-parity band in ^{44}Ti. These members are expected at excitation energies above the α-threshold energy, which is not a well-known energy region. In addition, the

positive-parity band is investigated in the present experiment.

II. EXPERIMENTAL PROCEDURES AND RESULTS

A 50-MeV $^6Li^{2+}$ beam was provided by the isochronous cyclotron at the Research Center for Nuclear Physics (RCNP) of Osaka University. The beam current on the target was between 20 and 40 *e* nA. Deuterons emitted from the reaction (^{6}Li,*d*) were analyzed with the spectrograph RAIDEN.[26] The spectrograph acceptance angle of 0.5° in the scattering plane was used with the resultant solid angle of 1.7 msr. The observed overall resolution for the system was bout 50 keV full width at half maximum. Deuteron particles were detected and identified by the focal plane counter system consisting of a position-sensitive proportional counter of 1.5 m in length, two ΔE gas proportional counters, and an E plastic scintillation counter.[27] An enriched (99.8%) ^{40}Ca target, with thickness of 200 μg/cm^2, was prepared by evaporation onto a gold foil backing and was fixed in a scattering chamber without exposure to air. Data were taken with three or four separate settings of the spectrograph magnetic field in order to cover the entire excitation energy region of $E_x = 0-13$ MeV. Angular distributions for 34 levels were obtained at intervals of 2.5° for $\theta_{lab} = 5°-20°$ and 5° for $\theta_{lab} = 20°-35°$. The upper and lower parts in Fig. 1 show the energy spectra of deuterons emitted from the reaction ^{40}Ca(^{6}Li,*d*)^{44}Ti at $\theta_{lab} = 6°$ for levels below and above the α-threshold energy, respectively. Contaminant peaks from the reaction (^{6}Li,*d*) on the light impurities of C and O were identified from the kinematic shift of the spectra line with the angle of observation. The observed excitation energies of the levels in ^{44}Ti were in agreement within 30 keV of the results obtained from the data at $E = 32$ MeV by Strohbusch *et al.*[18] The excitation energies labeled in Fig. 1 were in accordance with Ref. 18. Furthermore, additional levels were identified in the present experiment (see Table II). As reported in a previous paper,[28] the 11.7-MeV 1^- state which has been identified by Frekers *et al.*[20,21] was not clearly excited in the present experiment.

Figures 2 and 3 display angular distributions obtained at $E = 50$ MeV. These angular distributions exhibit shapes which are characteristic of the transferred orbital angular momentum. The curves present the results of α-transfer distorted-wave Born approximation (DWBA) calculations normalized to the experimental data to deduce the α-spectroscopic factors S_α.

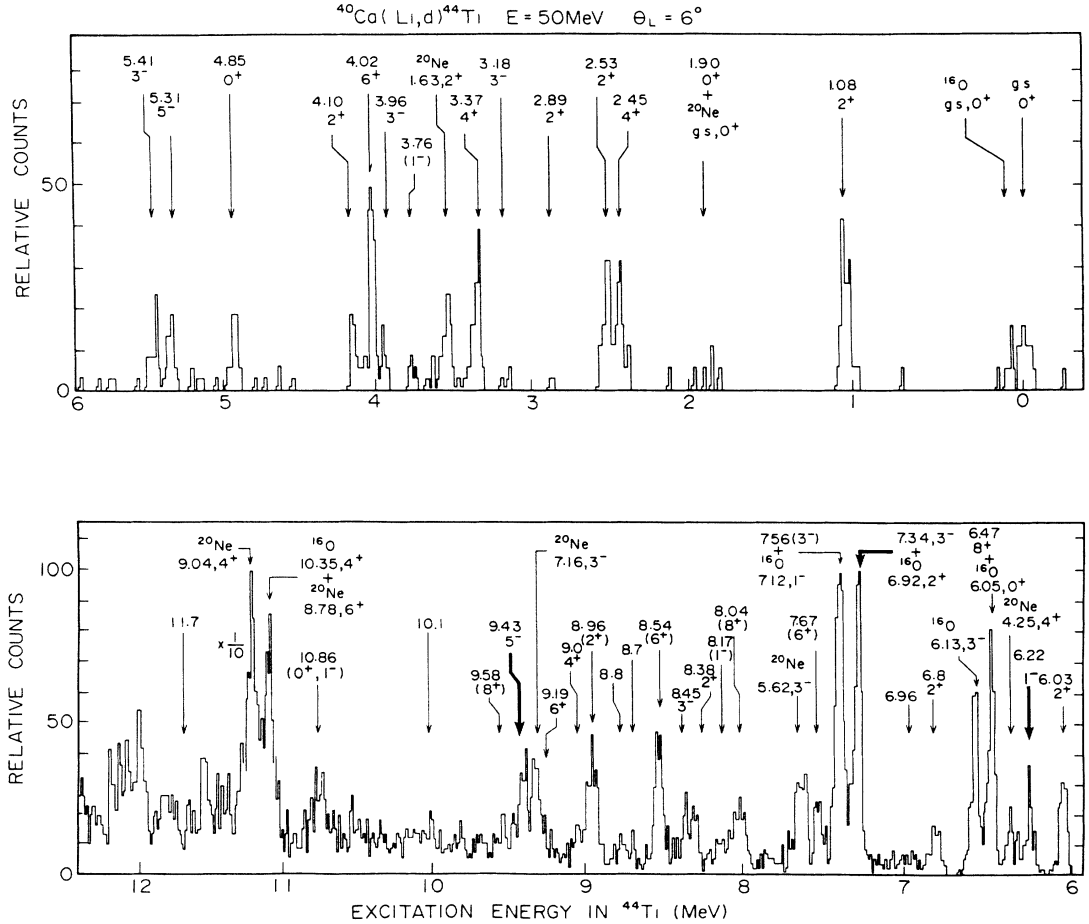

FIG. 1. Deuteron spectra to the excited states below and above the α-threshold energy. The peaks assigned as the negative-parity band in the present work are indicated by the strong arrows. The 7.34-MeV state assigned to $L = 3$ transfer is mixed with the 6.92-MeV 2^+ state of ^{16}O at this angle.

III. ANALYSES

The angular distributions were analyzed using the finite-range DWBA code TWOFNR and TWOFNREX (Ref. 29) to determine the transferred angular momentum L. According to the DWBA calculations, the α-particle transfer in the (^{6}Li,d) and (d,^{6}Li) (Refs. 30 and 31) reactions occur at a local radius of the nuclear surface where amplitudes of the overlap integral in the reactions show a sharp maximum related to only a few partial distorted waves. This feature suggests that the DWBA analysis is a good approximation for α-transfer reactions. Furthermore, as seen in Fig. 2, the characteristic shapes of the angular distributions indicate the dominance of a direct-reaction process, which describes an α-particle-transfer mechanism for each allowed angular momentum transfer. Considering that the DWBA analysis is a good approximation for the (^{6}Li,d) reaction, optical-model potential parameters obtained from the analyses of the elastic-scattering data are nearly expected as the appropriate parameters for the DWBA calculations.

The wave function of relative motion between the d and α clusters in the ground state of ^{6}Li has been well investigated.[32–34] Kubo and Hirata[35] looked for an analytic representation of the Wood-Saxon potential shape which was expressed in the effective interaction $V_{d\alpha}$ obtained from the phase shift of the $d+\alpha$ scattering. They found $V_{d\alpha}=72$ MeV as the depth of a potential with the

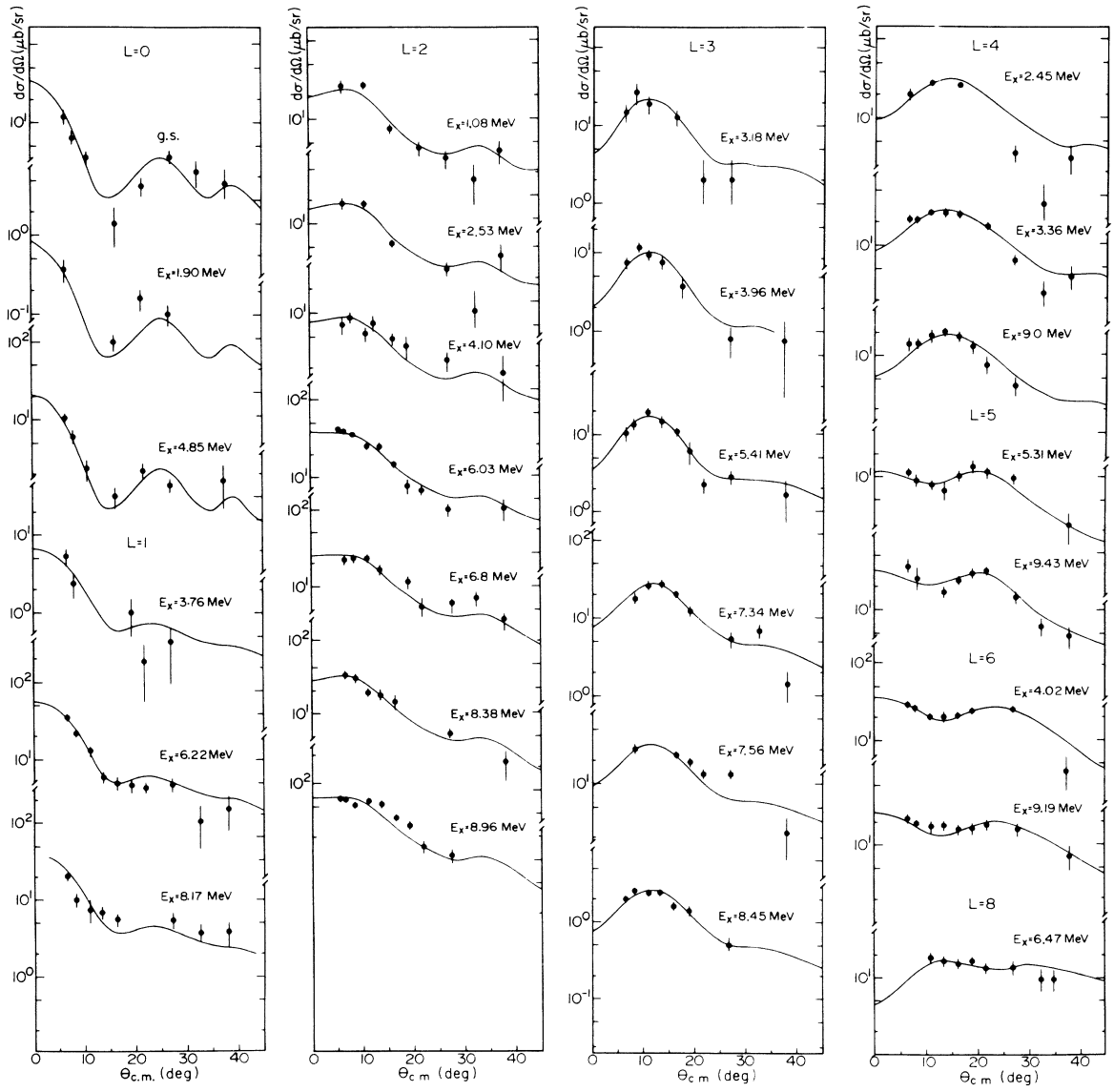

FIG. 2. Angular distributions of the $N=12$ and 13 states. The curves are the results of the finite-range DWBA calculations.

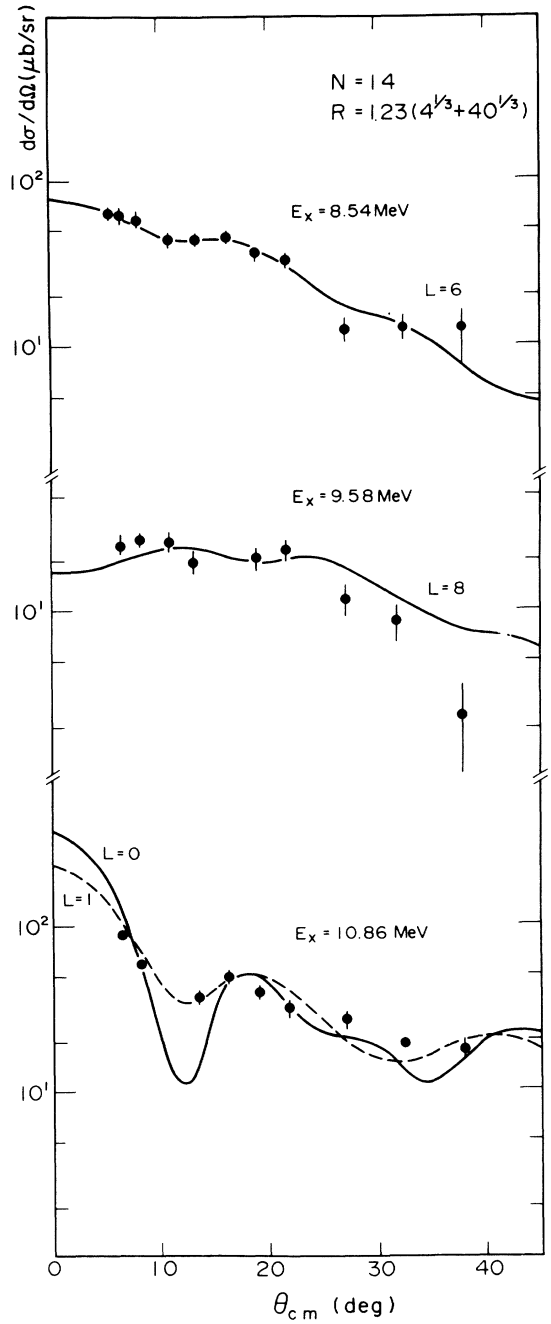

FIG. 3. Angular distributions of the strongly excited levels with $N=14$ and 15. The curves are the results of the finite-range DWBA calculations.

radius parameter $r_0=1.2$ fm and the diffuseness parameter $a=0.65$ fm, where $R=r_0 A_{\text{core}}^{1/3}$. In the present analyses, the potential depth $V_{d\alpha}$ was determined so as to give the separation energy $\text{SE}(d+\alpha)=1.47$ MeV, the node $n=1$, and the orbital angular momentum $l=0$ for the relative motion of two clusters in the ground state of ^{6}Li. The subsequent value obtained was $V_{d\alpha}=78$ MeV with $r_0=1.2$ fm and $a=0.65$ fm.

In the reaction channel, a role of the distorted waves inside the target nucleus is not exactly the same as one in the elastic scattering channel. Thus the distorted waves obtained from the elastic-scattering data are not invariably correct inside the nucleus for the reactions. The optical-model potential parameters obtained from the analyses of elastic-scattering data were used as a first guess in the DWBA calculations. The deuteron optical-model parameters were obtained from an analysis of deuteron elastic scattering at $E=52$ MeV by Hinterberger *et al.*[36] For the ^{6}Li optical-model potential, we adopted the potential parameters obtained from the analyses of ^{6}Li elastic scattering at $E=50.6$ MeV by Chua *et al.*[37] In the present DWBA calculations, the radius parameters of the deuteron and ^{6}Li real potentials were varied to obtain a good fit to the angular distributions of the fixed spin-parity states in ^{44}Ti. The deuteron spin-orbit potential plays a certain role in reproducing the angular distributions of the $(d,^6\text{Li})$ (Ref. 31) and $(^6\text{Li},d)$ reactions. In the $(^6\text{Li},d)$ reaction, the smaller spin-orbit potential depth than those for the elastic scattering and $(d,^6\text{Li})$ reaction was necessary to get better fits to the data. The spin-orbit potential of ^{6}Li was derived from the empirical deuteron spin-orbit potential using a folding model.[38] However, this part of the ^{6}Li optical potential has a minor effect on reproducing the experimental angular distributions. The optical-model parameters used in the present analysis are shown in Table I in comparison with those obtained from the elastic scatterings together with those used in the $(d,^6\text{Li})$ reaction.[31]

The bound-state wave functions for the transferred α cluster in ^{44}Ti were calculated using a Woods-Saxon well. The radius of the potential well was set equal to $R=1.0(40^{1/3}+4^{1/3})$ fm with a diffuseness parameters of 0.65 fm in the primary quantum number $N=2n_r+L=12$ and 13 states, where n_r and L denote the number of radial nodes and orbital angular momentum, respectively, of the α-particle wave functions. In the case of the $^{40}\text{Ca}+\alpha$ system, the states with $N=12$ correspond to the

TABLE I. Optical-potential parameters. The radii are defined as $R_x=r_x A_T^{1/3}$ fm, where A_T is the target mass number, and the Coulomb radius is taken to be $R_C=1.40A_T^{1/3}$ fm for d and ^{6}Li channels.

	V_R (MeV)	r_R (fm)	a_R (fm)	W_I^V (MeV)	W_I^S (MeV)	r_I (fm)	a_I (fm)	V_{so} (MeV)	r_{so} (fm)	a_{so} (fm)
d channel										
elastic	88.9	1.05	0.85		11.7	1.3	0.779	7.0	1.05	0.85
$(d,^6\text{Li})$	88.9	1.35	0.85		11.7	1.3	0.779	5.0	1.05	0.85
$(^6\text{Li},d)$	88.9	1.35	0.85		11.7	1.3	0.779	3.5	1.05	0.85
^{6}Li channel										
elastic	244	1.30	0.7	23.5		1.70	0.9			
$(d,^6\text{Li})$	244	1.30	0.7	23.0		1.70	0.9	2.0	1.0	0.9
$(^6\text{Li},d)$	244	1.05	0.7	23.5		1.70	0.9	2.0	1.0	0.9

positive-parity band states and the states with $N=13$ correspond to the negative-parity band states. Potential depths were adjusted to reproduce the α-separation energy. For the unbound states, the wave functions are those which correspond to weak binding energy $E_B=-0.1$ MeV.

At first, the calculations of the cross sections up to $L=10$ for the $N=12$ and 13 states were performed. The angular distributions obtained using these calculations are indicated by the solid curves in Fig. 2. It is evident that the results of the DWBA calculations for the known spin states with $J^\pi=0^+-8^+$ well reproduce the data. The $J^\pi=8^+$ state at $E_x=6.47$ MeV corresponds to the state at $E_x=6.508$ MeV by Simpson *et al.*[25] The angular distributions of the strongly excited states at 8.54 and 10.86 MeV as well as the more weakly populated state at 9.58 MeV were not reproduced by the calculations for any transfer angular momentum L allowed for $N=12$ or 13 states. These angular distributions are shown in Fig. 3 together with the calculated curves. Considering higher nodal states, the calculations with $N=14$ were performed with a radius $R=1.23(40^{1/3}+4^{1/3})$ fm for these levels. In general, a single-particle orbit in the harmonic-oscillator potential expands its radius with increasing primary quantum number N.[39] Such a property of the single-particle wave function may be not lost in the Woods-Saxon potential. In the present case, the bound-state wave functions for the transferred α cluster were calculated using a potential with a Woods-Saxon shape, and it may be reasonable to assume that the radius parameters of the wave functions with $N=14$ should be larger than those with $N=12$. The angular distributions calculated with $L=6$ and 8 as $N=14$ states reproduced the data of the 8.54- and 9.58-MeV states, respectively. For the state at 10.86 MeV, either results of the calculations for $L=0$ ($N=14$) or $L=1$ ($N=15$) reproduced the data (see Fig. 3). However, a unique angular momentum transfer for this state could not be determined.

IV. DISCUSSION

A. Positive-parity band states

In Table II we present a summary of the results of the present analyses compared with the known levels[18,19,21–25,40] in ^{44}Ti. The spin parities obtained from the present analysis are in good agreement with those of the known levels. It is suggested that the characteristic angular distributions in the present experiment indicate dominance of a direct-reaction process, which enables an identification of the spin parity of states assuming an α-particle-transfer reaction. As seen in Fig. 2, the calculated curve for the 8^+ state at 6.47 MeV (corresponding to the 6.508-MeV state in Ref. 25) also well reproduces the data. This state is unbound in the ^{40}Ca+α system, and this fact supports the use of an unbound wave function approximated in the (^{6}Li,d) reaction by a wave function corresponding to a weak binding energy. The Coulomb barrier height in the system ^{40}Ca+α is about 11 MeV, which corresponds to 16 MeV of excitation energy in ^{44}Ti. A state with an internal wave function at a few MeV above the α-threshold energy may drop steeply at the nuclear surface due to the Coulomb barrier and behave like a bound-state wave function with a weak binding energy. Angular distributions of some levels near 4 MeV above α-threshold energy are also in agreement with the DWBA calculations for the appropriate angular momentum transfer L of the $N=12$ and 13 states.

For the strongly excited level at 8.54 MeV, which was tentatively assigned as $J^\pi=0^+$ by the study at $E=32$ MeV,[18] there was no DWBA calculation for the range of L allowed with $N=12$ and 13 that reproduced the fall of cross sections at large backward angles. The calculation for $L=6$ of the $N=14$ state, however, reproduces the data, if a radius parameter of the α-wave function in ^{44}Ti is taken as $R=1.23(40^{1/3}+4^{1/3})$ fm (see Fig. 3). The cross sections of an $N=14$ state with such a large angular momentum transfer falls at backward angles, and in spite of very small α-cluster amplitudes in ^{44}Ti, these states are sometimes strongly excited. In fact, since the wave functions of these states extend to outer side of the nuclear surface, the amplitudes of the overlap integral for the α transfer are large. The 9.58-MeV level, which is not so strongly excited, may also be a state with $N=14$. The 10.86-MeV level is strongly excited. The results of the DWBA calculations for either $L=0$ or 1 well reproduce the angular distribution of this level, with spectroscopic factors of 0.25 and 0.10 for $L=0$ and 1, respectively. These values are much larger than those of the $N=12$ and 13 states. According to the theoretical calculation based on an α-cluster model,[5–8] this level corresponds to a band head of higher nodal states of either an $N=14$ positive-parity or $N=15$ negative-parity band.

Angular distributions of the members of the positive-parity band ($N=12$), which is terminated at 8.04 MeV, are shown in Fig. 4. The results of the DWBA calculations for the states of $J^\pi=0^+$, 2^+, 4^+, 6^+, and 8^+ are in good agreement with the data. The spectroscopic factors range from 0.03 to 0.04 for these states. For the 7.67-MeV 10^+ state, however, there is a large discrepancy between the experimental and theoretical cross sections at the backward angles (the DWBA calculation for $L=12$ transfer is impossible in the present codes). The shape of angular distributions of the 7.67-MeV 10^+ and 8.04-MeV 12^+ states are similar to that of the 8.54-MeV state. For the 7.67- and 8.04-MeV states, the DWBA calculations were performed as $N=14$ states using the weak-bound wave functions with $r_0=1.23$ fm for the 7.67-MeV state and 1.35 fm for the 8.04-MeV state, where $R=r_0(4^{1/3}+40^{1/3})$. The results are the dotted curves compared with the data in Fig. 4. The curves of $L=6$ and 8 for these states at 7.67 and 8.04 MeV seem to agree well with the data, and the deduced spectroscopic factors are less than 0.01. However, the present assignment for these two states are tentative. Considering the above results and the fact that the excitation energies of the states at 7.67 and 8.04 MeV are much too low as the $J^\pi=10^+$ and 12^+ states of the ground-state band with $N=12$, it is suggested that the wave functions of these states are somewhat different than those of the other states of the ground-state band.

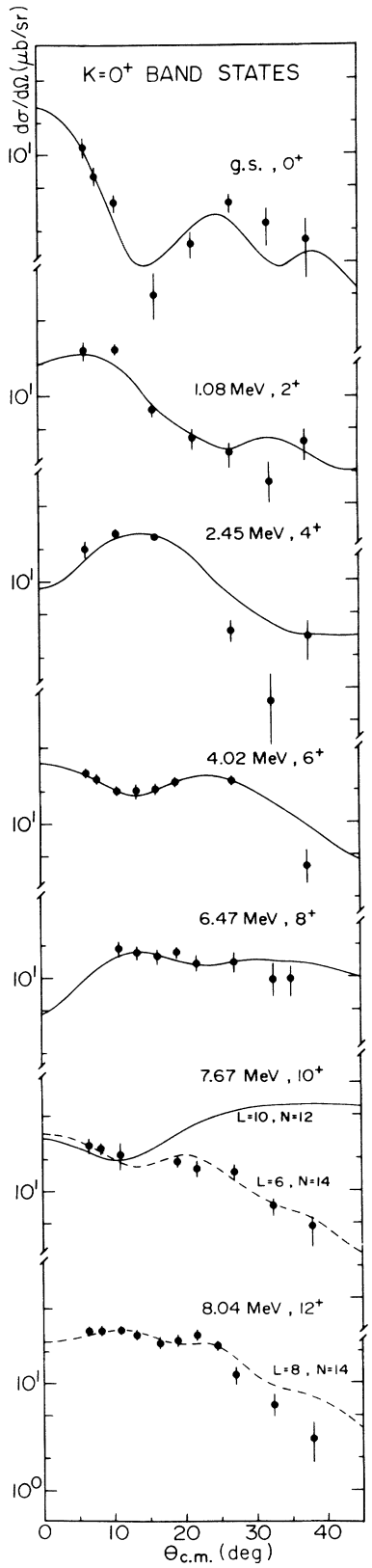

FIG. 4. Angular distributions of the members of the ground-state band (the positive-parity band, $K^{\pi}=0^{+}$). The solid and dashed curves indicate the results calculated as $N=12$ and 14 states, respectively.

B. Negative-parity band states

On the basis of the results of the DWBA analyses, the levels at 6.22, 7.34, and 9.43 MeV were assigned as $L=1$, 3, and 5 transition states, respectively. We can consider these three states as candidates for members of the negative-parity band with $N=13$ by comparing with the results of the theoretical calculations. These angular distributions are compared with the DWBA calculations in Fig. 5. Determination of the transferred angular momentum L for the 6.22-MeV state is difficult because the

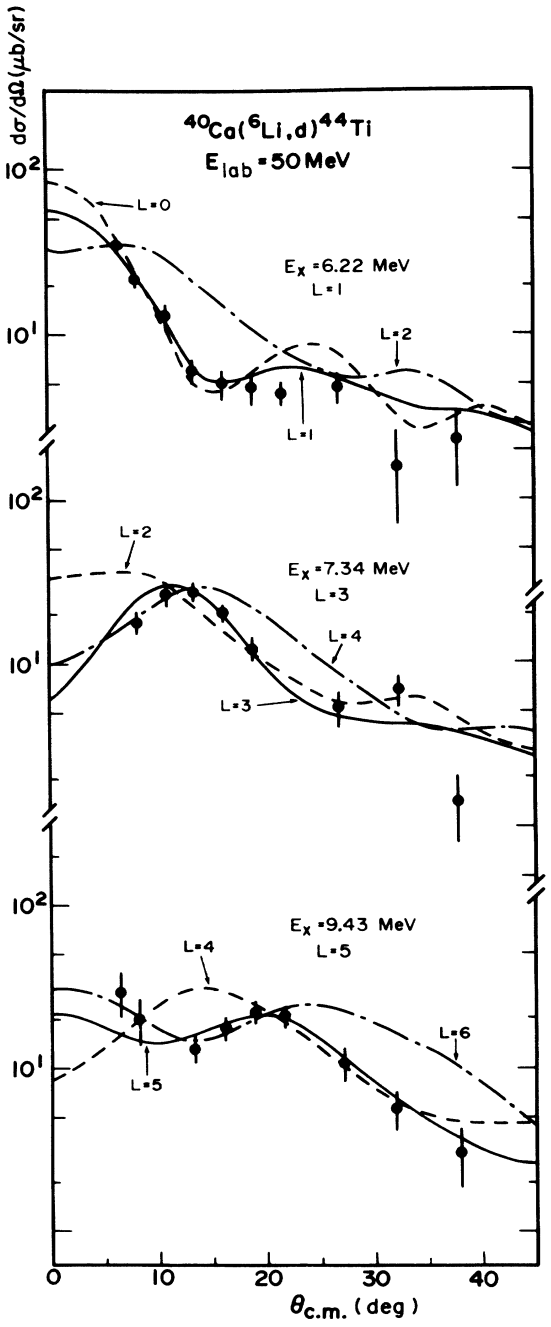

FIG. 5. Angular distributions of the 6.22-, 7.34-, and 9.43-MeV states at $E(^{6}\mathrm{Li})=50$ MeV. The solid curves indicate the best fit to the data by the DWBA calculations.

TABLE II. Levels in ^{44}Ti.

^{40}Ca(α,γ) (Refs. 22, 23, and 24)		^{32}S(^{14}N,$pn\gamma$) ^{28}Si(^{19}F,$p2n\gamma$) (Ref. 25)		^{46}Ti(p,t) (Ref. 39)		^{40}Ca(^{6}Li,d) $E=32$ MeV (Refs. 18, 19, and 21)		^{40}Ca(^{6}Li,d) $E=50$ MeV Present work		
E_x	J^π	E_x	J^π	E_x	J^π	E_x	J^π	E_x	J^π	S_α
g.s.	0^+	g.s.	0^+	g.s.	0^+	g.s.	0^+	g.s.	0^+	0.04
1.083	2^+	1.083	2^+	1.82	2^+	1.08	2^+	1.08	2^+	0.03
1.904	0^+			1.903	0^+	1.90	0^+	1.90	0^+	<0.01
2.454	4^+	2.454	4^+	2.450	(4^+)	2.44	4^+	2.45	4^+	0.03
2.530	2^+			2.535	(2^+)	2.52	2^+	2.53	2^+	0.02
2.886	2^+			2.885	2^+			2.89	2^+	0.002
3.175	(3^-)	3.176	(3^-)	3.175	(2^+)			3.18	3^-	0.002
3.364	4^+			3.365	4^+	3.35	4^+	3.37	4^+	0.03
3.415	3^+									
3.645	(4^-)	3.645	(4^-)					(3.64)		
3.775	(2^+)					(3.74)		3.76	(1^-)	0.005
3.942	(3^-)			3.942	3^-	3.92		3.96	3^-	0.005
3.980	4^+			3.980	4^+					
4.015	6^+	4.015	6^+	4.015	$(5^-,6^+)$	4.00	>4	4.02	6^+	0.03
4.061	$(5^-,3^-)$	4.060	(5^-)	4.060	4^+					
4.116	2^+					4.10	2^+	4.10	2^+	0.007
4.227										
4.792				4.605	0^+					
				4.792	(2^+)					
						4.84	0^+	4.85	0^+	0.02
				5.055	(4^+)	5.08				
5.305				5.315		5.23				
						5.33	(4^+)	5.31	5^-	0.009
5.423				5.415	(2^+)	5.41		5.41	3^-	0.01
				6.030	(4^+)	6.03		6.03	2^+	0.04
						6.22		6.22	1^-	0.04
						6.47		6.47	8^+	0.04
6.508	(8^+)	6.508	(8^+)							
				6.535						
				6.600	$2^+,T=1$					
								6.8	2^+	0.02
				6.965	$4^+,T=1$			6.96		
7.216	$1^+,T=1$					7.21				
						7.34		7.34	3^-	0.03
						7.56		7.56	(3^-)	0.02
7.671	(10^+)	7.671	(10^+)	7.670	(4)	7.67		7.67	(6^+)	0.006
8.039	(12^+)	8.039	(12^+)			8.04	≥ 6	8.04	(8^+)	0.002
								8.17	(1^-)	0.015
						8.38		8.38	2^+	0.03
								8.45	3^-	0.002
						8.54	(0^+)	8.54	(6^+)	0.003
								8.7		
								8.8		
						(8.96)		8.96	(2^+)	0.06
						(9.03)		9.0	4^+	0.02
								9.19	6^+	0.02
9.338	$0^+,T=2$			9.330	$0^+,T=2$					
9.427	(4^+)					9.43		9.43	5^-	0.03
						9.58		9.58	(8^+)	0.003
9.698	2^+									
9.713	(4^+)									
9.908	$2^+,3^-$									
	$4^+,5^-$									
10.129	(1,2)									
10.209	≤ 2									
10.386	$(2^+,3^-)$									

TABLE II. (*Continued*).

^{40}Ca(α,γ) (Refs. 22, 23, and 24)		^{32}S(^{14}N,$pn\gamma$) ^{28}Si(^{19}F,$p2n\gamma$) (Ref. 25)		^{46}Ti(p,t) (Ref. 39)		^{40}Ca(^{6}Li,d) $E=32$ MeV (Refs. 18, 19, and 21)		^{40}Ca(^{6}Li,d) $E=50$ MeV Present work		
E_x	J^π	E_x	J^π	E_x	J^π	E_x	J^π	E_x	J^π	S_α
						10.44				
						10.86		10.86	(0^+)	0.25
									(1^-)	0.10
						11.69	1^-			
						12.2				

difference between the shape of the angular distribution for $L=0$ and 1 is not definitive at $E=50$ MeV. However, the calculated angular distributions for any transferred L larger than 1 does not reproduce the present data. Fortunately, the angular distribution of this state measured at $E=28$ MeV has been reported by Fulbright *et al.*[19] over the angular range $=10°-70°$. An angular distribution at such a lower incident energy is more sensitive in identifying lower angular momentum transfers. In Fig. 6 the results of the present analysis for the angular distributions of the 6.22-MeV and ground states obtained from Ref. 19 are shown. The calculated curves were obtained by using the same optical potential parameters as those presented in Table I. The present analysis shows that the DWBA curve for an $L=0$ transfer well reproduces the angular distribution of the 0^+ ground state. The curve for the $L=1$ transfer is in good agreement with the data of the 6.22-MeV state. The spectroscopic factor deduced from the data at $E=28$ MeV is 0.04 and is in agreement with the result obtained from the present data at $E=50$ MeV. Consequently, it is evident that the DWBA curve for $L=1$ is most suitable to fit the angular distribution of the 6.22-MeV state. For the 7.34-MeV state, the calculated angular distribution for the $L=3$ transfer (shown in the middle of Fig. 5) fits the data very well. The data points of the 9.43-MeV state include some ambiguity at angles smaller than 10° because of an ^{16}O contaminant peak in the spectra. Nevertheless, the calculated curve for the $L=5$ transfer well reproduces the data at the angles larger than 15°, while neither the $L=4$ nor 6 curve reproduces the data as shown in the bottom of Fig. 5. On the basis of this DWBA analysis, it is indicated that the spin and parity of the 6.22-, 7.34-, and 9.43-MeV states are 1^-, 3^-, and 5^-, respectively.

V. SUMMARY AND CONCLUSIONS

The general advantages and disadvantages of the (^{6}Li,d) and (d,^{6}Li) reactions have been described in Ref. 41. In the present experiment, spin assignment characteristics of a favorable L transfer in the reaction (^{6}Li,d) on ^{40}Ca were determined for the $N=12$ and 13 states of ^{44}Ti. For unbound wave functions at excitation energies above the α threshold, which is sufficiently below the Coulomb barrier in the system ^{40}Ca$+\alpha$, weak binding energy is a useful assumption.

Recently, the results of several theoretical calculations[5-8] have shown that α-cluster structure persists in the ^{44}Ti nucleus, including the ground-state band. In Fig. 7, the parity doublet energy levels observed in the present experiment are compared with those predicted by α-cluster model calculations.[5-8] The predicted energy levels of the α-cluster negative-parity band, starting just above the α threshold, correspond well to those of the observed levels (indicated by thick lines in Fig. 7).

It is interesting to compare the α-cluster strength of the negative-parity states with those of the positive-parity states. It should be noted that the spectroscopic factors deduced from the present data are for unbound states. Thus the α-wave function used in the DWBA calcula-

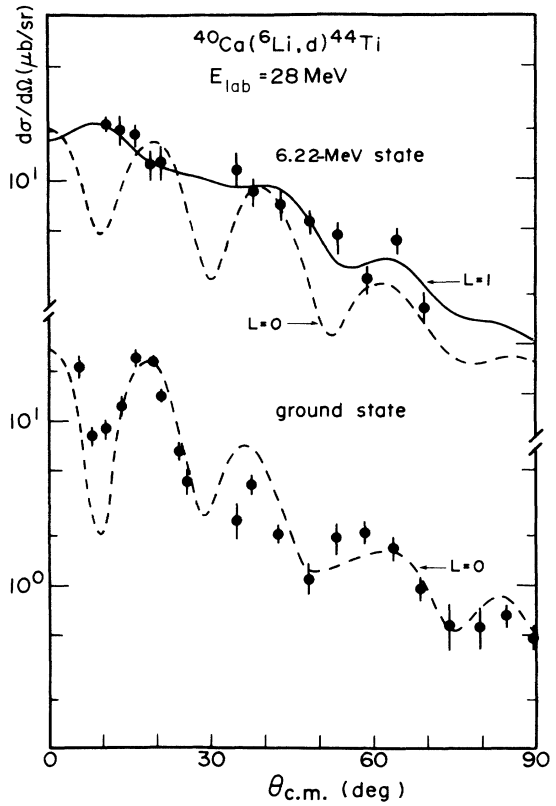

FIG. 6. Angular distributions of the ground state and 6.22-MeV state at $E(^{6}\text{Li})=28$ MeV by Fulbright *et al.* (Ref. 19). The dashed and solid curves indicate the $L=0$ and 1 transfer, respectively. For the 6.22-MeV state, the $L=1$ curve well reproduces the data.

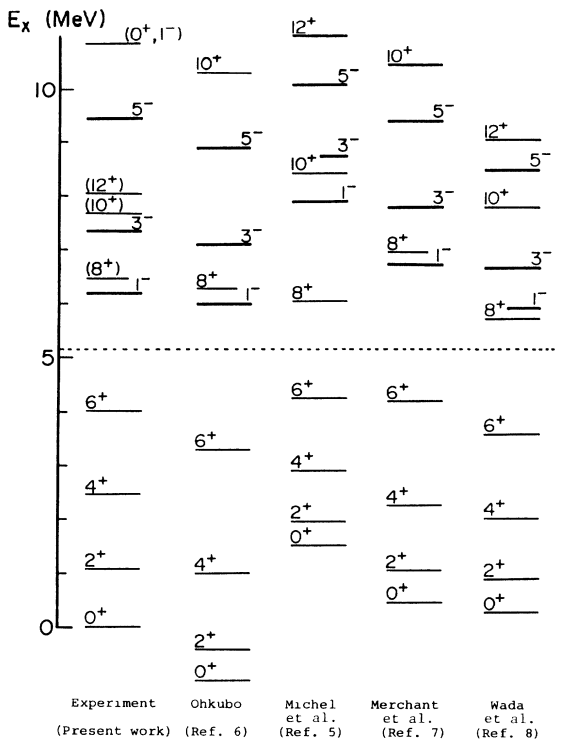

FIG. 7. Observed parity doublet band in comparison with the theoretical predictions of α-cluster states in ^{44}Ti. The negative-parity states observed in the present experiment are indicated by thick lines. The 10.86-MeV state is a candidate of the bandhead of the higher nodal state of $N=14$ or 15.

tions are those for which weak binding energy $E_B=-0.1$ MeV was assumed. In the present reaction, the change in shape of the angular distribution with change in the binding energy for the wave functions is minor, but the change in the magnitude of the cross sections may not be negligible. For these wave functions, the relative spectroscopic factors S_α/S_α(g.s.) of 1.0, 0.75, and 0.75 were deduced from the present data for the 1^-, 3^-, and 5^- states, respectively. In this case, the value of the spectroscopic factor for the ground state was S_α(g.s.)=0.04, where the $S_{d\alpha}$ was assumed to be 1.0 for the $2s$ relative state in the $d+\alpha$ system of ^{6}Li.

Furthermore, the strongly excited level at 10.86 MeV is assigned to be either a $J^\pi=0^+$ or 1^- state with $N=14$ or 15. This state has a large spectroscopic factor, and is a candidate of the bandhead of the higher nodal state for $N=14$ or 15.

In conclusion, using the (^{6}Li,d) transfer reaction at 50 MeV, we have shown the presence of a negative-parity band starting just above the α-threshold energy. These negative-parity members excited at such a low-lying energy region cannot be described by a single-particle shell model. The observations of the parity doublet band predicted from a α-cluster picture in ^{44}Ti supports the existence of moleculelike structure in the fp-shell nuclei. The energy gap between the ground 0^+ state as the bandhead of the $K^\pi=0^+$ band and the 6.22-MeV 1^- states as that of the $K^\pi=0^-$ band is well explained by the α-cluster model. It is suggested that the ground-state band of ^{44}Ti has a considerable α-cluster component. On the basis of these results, it was found that nucleons in the ^{44}Ti nucleus heavier than $A=40$ form an α-particle structure in spite of the strong effects of the spin-orbit coupling force. It is, furthermore, expected to observe the negative-parity band predicted by the α-cluster theory for ^{40}Ca,[42,43] which is an analog of ^{16}O.

ACKNOWLEDGMENTS

We are grateful to Professor H. Horiuchi for his continuous encouragements during this experiment, and would like to thank Professor F. Michel and Dr. T. Yamada for many useful discussions. We also wish to thank Professor M. Yabe for his assistance in the DWBA calculations. We are also grateful to Professor P. E. Hodgson for valuable discussions. We are indebted to Professor M. B. Greenfield for reading the manuscript and his comments. This experiment was performed at RCNP under Program No. 27A25.

[1]H. Kihara, M. Kamimura, and A. Tosaki-Suzuki, in *Proceedings of the International Conference on Nuclear Structure, Tokyo, 1977,* edited by the Organizing Committee (International Printing, Tokyo, 1977), p. 235.
[2]A. A. Pilt, Phys. Lett. **73B**, 274 (1978).
[3]K. F. Pal and R. G. Lovas, Phys. Lett. **96B**, 19 (1980).
[4]H. Horiuch, Prog. Theor. Phys. **73**, 1172 (1985).
[5]F. Michel, G. Reidemeister, and S. Ohkubo, Phys. Rev. Lett. **57**, 1215 (1986); Phys. Rev. C **37**, 292 (1988).
[6]S. Ohkubo, Phys. Rev. C **38**, 2377 (1988).
[7]A. C. Merchant, K. F. Pal, and P. E. Hodgson, J. Phys. G **15**, 601 (1989).
[8]T. Wada and H. Horiuchi, Phys. Rev. C **38**, 2063 (1988).
[9]D. A. Bromley, in *Proceedings of the Fourth International Conference on Clustering Aspects of Nuclear Structure and Nuclear Reaction, Chester, 1984,* edited by J. S. Lilley and M. A. Nagarajan (Reidel, Dordrecht, 1985), p. 1; see also references therein.
[10]H. Horiuchi and K. Ikeda, Prog. Theor. Phys. **40**, 277 (1968).
[11]A. M. Friedman, H. T. Fortune, G. C. Morrison, and R. H. Siemssen, in *Proceedings of the International Conference on Nuclear Reaction Induced by Heavy Ion, Heihderberg, Germany, 1969,* edited by R. Bock and W. R. Hering (North-Holland, Amsterdam, 1970), p. 171.
[12]H. Faraggi, M. C. Lemaire, J.-M. Loiseaux, M. C. Mermaz, and A. Papineau, Phys. Rev. C **4**, 1375 (1971).
[13]G. C. Morrison, J. Phys. (Paris) Colloq. **32**, C-26 (1971).
[14]J. R. Erskine, W. Henning, and L. R. Greenwood, Phys. Lett. **47B**, 335 (1973).
[15]R. H. Siemssen, C. L. Fink, L. R. Greenwood, and H. J. Korner, Phys. Rev. Lett. **28**, 626 (1971).
[16]R. H. Siemssen, M. L. Halbert, M. Saltmarsh, and A. van der

Woude, Phys. Rev. C **4**, 1004 (1971).
[17]V. Z. Goldberg, V. V. Davydov, A. A. Oglobin, S. B. Sakuta, and V. I. Chuev, Izv. Akad. Nauk. SSSR, Ser. Fiz. **33**, 586 (1969) [Bull. Acad. Sci. USSR, Phys. Ser. **33**, 542 (1970)].
[18]U. Strohbush, C. L. Fink, B. Zeidman, R. G. Markham, H. W. Fulbright, and R. N. Horoshko, Phys. Rev. C **9**, 965 (1974).
[19]H. W. Fulbright, C. L. Bennett, R. A. Lindgren, R. G. Markham, S. C. McGuire, G. C. Morrison, U. Strohbush, and J. Toke, Nucl. Phys. **A284**, 329 (1977).
[20]D. Frekers, H. Eickhoff, H. Lohner, K. Poppensieker, R. Santo, and C. Wiezorek, Z. Phys. A **276**, 317 (1976).
[21]D. Frekers, R. Santo, and K. Langanke, Nucl. Phys. **A394**, 289 (1983).
[22]W. R. Dixon, R. S. Storey, and J. J. Simpson, Nucl. Phys. **A202**, 579 (1973).
[23]J. J. Simpson, W. R. Dixon, and R. S. Storey, Phys. Rev. Lett. **31**, 946 (1973).
[24]W. R. Dixon, R. S. Storey, and J. J. Simpson, Phys. Rev. C **15**, 1896 (1977).
[25]J. J. Simpson, W. Dunnweber, J. P. Wurm, P. W. Green, J. A. Kuehner, W. R. Dixon, and R. S. Storey, Phys. Rev. C **12**, 468 (1975); J. J. Kolata, J. W. Olness, and E. K. Warburton, *ibid.* **10**, 1663 (1974).
[26]H. Ikegami, S. Morinobu, I. Katayama, M. Fujiwara, and S. Yamabe, Nucl. Instrum. Methods. **175**, 335 (1981).
[27]Y. Fujita, K. Nagayama, M. Fujiwara, S. Morinobu, T. Yamazaki, and H. Ikegami, Nucl. Instrum. Methods **217**, 441 (1983).
[28]T. Yamaya, S. Oh-ami, O. Satoh, M. Fujiwara, S. Hatori, T. Itahasi, K. Katori, S. Kato, M. Tosaki, and S. Ohkubo, Phys. Rev. C **41**, 2421 (1990).
[29]M. Igarashi, finite-range DWBA codes TWOFNR and TNOFNREX (private communication).
[30]T. Yamaya, K. Umeda, T. Suehiro, K. Takimoto, R. Wada, E. Takada, M. Fukada, J. Shimizu, and Y. Ohkuma, Phys. Lett. **90B**, 219 (1980).
[31]K. Umeda, T. Yamaya, T. Suehiro, K. Takimoto, R. Wada, E. Takada, S. Shimoura, A. Sakaguchi, T. Murakami, M. Fukada, and Y. Ohkuma, Nucl. Phys. **A429**, 88 (1984).
[32]A. Hasegawa and S. Nagato, Prog. Theor. Phys. **38**, 118 (1967).
[33]J. L. Gammel, B. J. Hill, and R. M. Thaler, Phys. Rev. **119**, 267 (1960).
[34]M. B. Greenfield, M. F. Werby, and R. J. Philpott, Phys. Rev. C **10**, 564 (1974).
[35]K.-I. Kubo and M. Hirata, Nucl. Phys. **A187**, 186 (1972).
[36]F. Hinterberger, G. Mairle, U. Schmidt-Rohr, G. J. Wagner, and P. Turek, Nucl. Phys. **A111**, 265 (1968).
[37]L. T. Chua, F. D. Becchetti, J. Janecke, and F. L. Milder, Nucl. Phys. **A237**, 243 (1976).
[38]W. J. Thompson, in *Proceedings of the International Conference on Reactions between Complex Nuclei, Nashville, 1974,* edited by R. L. Robinson, F. K. McGowan, J. B. Ball, and J. H. Hamilton (Elsevier, New York, 1974), Vol. 1, p. 14.
[39]A. Bohr and B. R. Mottelson, *Nuclear Structure* (Ben, New York, 1969), Vol. 1, p. 220.
[40]J. Rapaport, J. B. Ball, R. L. Auble, T. A. Belote, and W. E. Dorenbusch, Phys. Rev. C **5**, 453 (1972).
[41]F. D. Becchetti, in *Proceedings of the Third International Conference on Clustering Aspects of Nuclear Structure and Nuclear Reactions, Winnipeg, Manitoba, Canada, 1978,* AIP Conf. Proc. No. 47, edited by W. T. H. Van Oers, J. P. Svenne, J. S. C. McKee, and W. R. Falk (AIP, New York, 1978), p. 308.
[42]S. Ohkubo and K. Umehara, Prog. Theor. Phys. **80**, 598 (1988).
[43]G. Reidemeister, S. Ohkubo, and F. Michel, Phys. Rev. C **41**, 63 (1990).